Metabolic Engineering 26 (2014) 57–66

Contents lists available at ScienceDirect

Metabolic Engineering

journal homepage: www.elsevier.com/locate/ymben

Evolution reveals a glutathione-dependent mechanism of 3-hydroxypropionic acid tolerance

Kanchana R. Kildegaard [a], Björn M. Hallström [b], Thomas H. Blicher [c], Nikolaus Sonnenschein [a], Niels B. Jensen [a,1], Svetlana Sherstyk [a], Scott J. Harrison [a], Jérôme Maury [a], Markus J. Herrgård [a], Agnieszka S. Juncker [a], Jochen Forster [a], Jens Nielsen [a,d], Irina Borodina [a,*]

[a] The Novo Nordisk Foundation Center for Biosustainability, Technical University of Denmark, Kogle Allé 6, DK-2970 Hørsholm, Denmark
[b] Science for Life Laboratory, KTH Royal Institution of Technology, Box 1031, SE-171 21 Solna, Sweden
[c] The Novo Nordisk Foundation Center for Protein Research, University of Copenhagen, Blegdamsvej 3b, DK-2200 Copenhagen , Denmark
[d] Department of Chemical and Biological Engineering, Chalmers University of Technology, Kemivägen 10, SE-412 96 Göteborg, Sweden

ARTICLE INFO

Article history:
Received 5 May 2014
Received in revised form
15 August 2014
Accepted 15 September 2014
Available online 28 September 2014

Keywords:
3-hydroxypropionic acid
Tolerance
3-hydroxypropionic aldehyde (reuterin)
Saccharomyces cerevisiae
Adaptive laboratory evolution

ABSTRACT

Biologically produced 3-hydroxypropionic acid (3HP) is a potential source for sustainable acrylates and can also find direct use as monomer in the production of biodegradable polymers. For industrial-scale production there is a need for robust cell factories tolerant to high concentration of 3HP, preferably at low pH. Through adaptive laboratory evolution we selected *S. cerevisiae* strains with improved tolerance to 3HP at pH 3.5. Genome sequencing followed by functional analysis identified the causal mutation in *SFA1* gene encoding S-(hydroxymethyl)glutathione dehydrogenase. Based on our findings, we propose that 3HP toxicity is mediated by 3-hydroxypropionic aldehyde (reuterin) and that glutathione-dependent reactions are used for reuterin detoxification. The identified molecular response to 3HP and reuterin may well be a general mechanism for handling resistance to organic acid and aldehydes by living cells.

1. Introduction

The carboxylic acid, 3-hydroxypropionic acid (3HP) is a potential platform chemical, which can be converted to a variety of valuable products such as acrylic acid, 1,3-propanediol, malonic acid, and building blocks for biodegradable polymers. Acrylic acid-derived products are used in diverse applications including super-absorbent polymers used in baby diapers and incontinence products, detergent polymers, various plastics, coatings, adhesives, elastomers, and paints. To date the market for acrylic acid and acrylic esters is around USD12 billion and it is predicted to grow at a rate of 3.7% annually. Acrylic acid has traditionally been derived from petrochemical feedstocks. Through fermentation with metabolically engineered microorganisms 3HP may be produced from renewable carbon sources, and further 3HP dehydration into acrylic acid represents an attractive alternative to the traditional acrylic acid production. Several methods for microbial production of 3HP have been developed during the last ten years (Kumar et al., 2013), where the most successful examples for 3HP production use *Escherichia coli* and *Klebsiella pneumonia* as the hosts and glucose and/or glycerol as substrates (Gokarn et al., 2007; Liao et al., 2010; Suthers and Cameron, 2006; Valdehuesa et al., 2013). We have developed baker's yeast, *Saccharomyces cerevisiae,* as an alternative host for 3HP production as this allows executing the process at low pH hereby ensuring direct production of 3HP acid (p*K*a 4.51) instead of salt, which makes the process more economically attractive (Chen et al., 2014).

The potential of microbial 3HP production has not yet been fully realized, as product toxicity represents a major bottleneck for industrial-scale production. Warnecke et al. (2008) applied multi-SCale Analysis of Library Enrichments (SCALES) approach (Lynch et al., 2007) and identified several genes and media supplements that individually or in combination were found to improve fitness of *E. coli* grown in continuous flow selections with increasing levels of 3HP . Based on the SCALES approach, 3HP toxicity was proposed

* Corresponding author. Fax: +45 4525 80 01.
E-mail address: irbo@biosustain.dtu.dk (I. Borodina).
[1] Present address: Evolva Biotech A/S, Lersø Park Allé 42-44, DK-2100 Copenhagen Ø, Denmark.

http://dx.doi.org/10.1016/j.ymben.2014.09.004

to be related to inhibition of the chorismate and threonine superpathways (Warnecke et al., 2010). Warnecke et al. (2012) also identified a small open reading frame in *E. coli* K12 (called *iroK*) encoding a 21-amino-acid peptide, which conferred 3HP tolerance. Despite the extensive research in *E. coli*, there have been no reports on improving 3HP tolerance in *S. cerevisiae*. Furthermore, the toxicity mechanism of 3HP is not understood at the molecular level.

One of the strategies to generate tolerance to specific chemicals and environmental stresses is laboratory evolution here referred to as adaptive laboratory evolution, which can result in genetic changes that are difficult if not impossible to predict rationally (Dragosits and Mattanovich, 2013). With recent progress in synthetic biology and in deep whole genome re-sequencing, it is possible to investigate the links between genotype and phenotype, and hereby the causal mutations in the evolved tolerant phenotypes can be identified and reverse engineered in the host (Dhar et al., 2011; Hong and Nielsen, 2012; Hong et al., 2011; Oud et al., 2012).

The aim of this work was to improve 3HP tolerance in yeast and to understand the mechanisms underlying 3HP toxicity and tolerance. Our strategy was to use adaptive laboratory evolution to generate 3HP tolerance and then to decipher the mechanism for 3HP tolerance by combination of whole-genome re-sequencing and transcriptome analysis to identify the relevant mutations that contribute to the phenotypic changes.

2. Material and methods

2.1. Strains and growth conditions

The yeast and bacterial strains used in this study are listed in Table S2. *S. cerevisiae* CEN.PK strains were obtained from Peter Kötter (Johann Wolfgang Goethe-University Frankfurt, Germany) and *E. coli* MG1655 was kindly provided by Adam Feist (University of California, San Diego). CEN.PK113-7D was used as a reference and a starting strain for the adaptive evolution approach, whereas CEN.PK113-32D was used as a parent strain for genetic engineering. Other yeasts and *E. coli* strains were used for studying the effect of glutathione (GSH) on 3HP tolerance. All standard cloning was carried out using *E. coli* strain DH5α.

Yeast strains were maintained on yeast peptone dextrose (YPD) medium at 30 °C for *S. cerevisiae* and at 25 °C for other yeast strains. *E. coli* strains were maintained on Luria-Bertani (LB) medium at 37 °C. *E. coli* transformants were selected on LB medium containing 100 μg ml^{-1} ampicillin. Growth test experiments for yeast and *E. coli* were performed in defined mineral medium and M9 medium, respectively. The composition of defined mineral medium was previously described (Jensen et al., 2014). For every 1 l of medium, 159 ml of 0.5 M citrate solution and 41 ml of 1 M Na_2HPO_4 solution were added into the concentrated defined mineral medium to maintain the pH at 3.5. For medium containing 3HP, the 3HP solution (ca. 30% in water, Tokyo Chemical Industry Co.) was neutralized with solid NaOH (0.133 g NaOH/1 ml of 3HP solution) and sterile-filtered before adding to the medium. Standard YPD and synthetic complete (SC) drop-out media were prepared from pre-mixed powders from Sigma-Aldrich. Most of the chemicals were obtained, if not indicated otherwise, from Sigma-Aldrich.

2.2. Adaptive evolution of CEN.PK113-7D

Three 3HP-tolerant strains were generated from CEN.PK 113-7D by a stepwise evolution approach for 200 generations on defined mineral medium (pH 3.5) containing 3HP. Specifically, a single colony of CEN.PK113-7D was inoculated into 5 ml YPD and grown with 200 rpm, overnight at 30 °C. The overnight culture was diluted in 50 ml fresh YPD to obtain the final OD_{600} of 0.5 and further incubated at 200 rpm, 30 °C for 5 h. The cells obtained from 50 ml YPD were used to inoculate three independent 250-ml shake flasks with baffles containing 20 ml of the same medium and supplemented with 25 g l^{-1} 3HP to an initial OD_{600} of 0.1. The adaptive evolution was carried out at 200 rpm, 30 °C until the exponential phase was reached and the cells were transferred to new fresh media. After the growth rate of the cultures has increased ($\approx$ 50 generations), the concentration of 3HP was increased to 50 g l^{-1} and the strains were further evolved for 34 days. Finally, ten single clones were isolated from each last shake flask and their growth rate on medium with 50 g l^{-1} 3HP was measured. As all the clones from the same evolution line showed identical behavior, we selected one clone from each evolution line for further characterization.

2.3. Physiological characterization of evolved strains

Batch cultivation of evolved strains was performed in biological triplicates on defined mineral medium (pH 3.5) with or without 50 g l^{-1} 3HP. Pre-cultures were prepared by inoculating a single colony from evolved and reference strains in 5 ml defined mineral medium (pH 3.5) and incubated at 200 rpm, 30 °C. After 24 h, the pre-cultures were inoculated into a 250-ml shake flask with baffles containing 40 ml of the same medium to a starting OD_{600} = 0.01. Batch cultivations of evolved strains grown on medium containing 50 g l^{-1} 3HP were performed as previously described except that pre-cultures were grown on medium containing 10 g l^{-1} 3HP. As the reference strain could not grow on 50 g l^{-1} 3HP, the batch cultivations were performed on medium containing 10 g l^{-1} 3HP instead. Batch cultivations were carried out in an orbital shaking incubator at 200 rpm and 30 °C. Cell growth was determined by measuring the absorbance at 600 nm wavelength. Glucose and primary metabolites were quantified using and Ultimate 3000 HPLC (Dionex, Sunnyvale, CA, USA) equipped with an Aminex HPX-87H ion exclusion column (300 mm × 7.8 mm, Bio-Rad Laboratories, Hercules, CA, USA) at 60 °C, using 5 mM H_2SO_4 as the mobile phase at a flow rate of 0.6 ml min^{-1}. Detection was performed using a Waters 410 Differential Refractometer Detector at 45 °C (Millipore Corp., Milford, MA), and a Waters 486 Tunable Absorbance Detector set at 210 nm.

2.4. Whole genome sequencing of 3HP evolved strains

The genomic DNA of evolved strains was isolated using QIAGEN Blood & Cell Culture DNA Kit (QIAGEN) according to the manufacturer's recommendation. Whole genome sequencing was performed on Illumina MiSeq at Science for Life Laboratory, KTH Royal Institution of Technology, Sweden. The DNA library for genome sequencing was prepared with the TruSeq DNA sample preparation kits and sequenced multiplexed in one 300-cycle run on an Illumina MiSeq, producing a total of 6.81 million assignable 2 × 150 bp read pairs. The raw reads were processed with the FastqMcf tool (http://code.google.com/p/ea-utils) in order to remove adapters and to clip poor quality ends (quality score < 20). Reads shorter than 50 bp after processing were discarded. The quality of the processed data was evaluated using FastQC (http://www.bioinformatics.bbsrc.ac.uk/projects/fastqc/) and passed all tests. Reads were mapped to the reference genome (CEN.PK 113-7D, http://cenpk.tudelft.nl) with MosaikAligner 2.1.32 (http://code.google.com/p/mosaik-aligner/) using a hash size of 11 bp. Indels were located and realigned with RealignerTargetCreator/IndelRealigner of Genome Analysis Toolkit (GATK) (McKenna et al., 2010). Duplicates were removed with the MarkDuplicates program of the Picard package (http://picard.sourceforge.net). Single nucleotide variants (SNVs) and small indels were detected using both GATK Unified Genotyper and Samtools mpileup/vcftools (Danecek et al., 2011; Li et al., 2009). The variant lists were filtered for all variants detected as homozygous for an alternative allele (different from the reference genome) in one or more of the samples. A total of 51 variants showed the exact same

variant in all four samples, and were discarded as errors in the reference sequence. The remaining 24 variants were manually inspected with Savant Genome Browser (Fiume et al., 2012), in order to discard obvious false positives. Large structural variation was detected from the mapped data using CNVnator 0.2.5 (Abyzov et al., 2011) and SVseq 2.0.1 (Zhang et al., 2012). A denovo approach was also performed where individual denovo assemblies were created with ABySS 1.3.4 (Simpson et al., 2009) and analyzed with the approach and helper scripts of the SOAPsv pipeline (Li et al., 2011). All methods found a number of structural variants present in all samples, caused by the incomplete or incorrect reference sequence (usually in repeated regions). All potential variants were inspected using the "Read Pair (Arc)" display mode of Savant Genome Browser.

2.5. Transcriptome analysis

Samples for RNA isolation were taken from the mid-exponential phase by rapidly sampling 25 ml of culture into a pre-chilled 50 ml tube with crushed ice. Cells were immediately centrifuged at 4 °C, 4000 rpm for 5 min. The supernatant was discarded and the pellets were resuspended in 2 ml of RNAlater® Solution (Ambion, Life Technologies) and incubated on ice for 1 h. The cells were pelleted by centrifugation at 12,000*g*, few seconds. The supernatant was discarded and the pellet was frozen in liquid nitrogen, and stored at −80 °C until further analysis. Total RNA extraction was performed using RNeasy® Mini Kit (QIAGEN). After thawing the samples on ice, 600 μl of buffer RLT containing 1% (v/v) β-mercaptoethanol was added directly to the cells. The mixture was transferred into a 2 ml extraction tube containing 500 μl glass beads. The cells were disrupted twice in the PRECELLYS®24 (Bertin Technologies) for 20 s at 6500 rpm. The cell mixture was pelleted and the supernatant was transferred to a new tube and total RNA was purified according to the manufacturing's protocol. The DNA was removed from the RNA samples using Turbo DNA-free™ Kit (Ambion). The quantity and quality of the RNA samples were measured using NanoPhotometer (Implen) and Agilent 2100 Bioanalyzer using the RNA 6000 Nano Assay (Agilent Technologies), respectively. The RNA samples were stored at −80 °C.

Transcriptome data was generated at the Center for Biological Sequence Analysis, Technical University of Denmark. cDNA synthesis and labeling were carried out according to Low Input Quick Amp Labeling Kit (One-color) manual (Agilent). Hybridization was performed using the NimbleGen Arrays containing probes for 5777 *S. cerevisiae* genes (Roche) and scanning with the NimbleGen MS 200 Microarray scanner.

The pre-processing and statistical analysis of the array data was performed in the R statistical environment. The pdInfoBuilder and oligo packages were applied for primary data handling and pre-processing, where the Robust Multichip Average (RMA) method was chosen for normalization and calculation of log 2 transformed expression indices. The org.Sc.sgd.db package, which is primarily based on ORF identifiers from SGD, was used to annotate the 5777 *S. cerevisiae* genes.

The gene expression values were compared between the reference strain (Ref) and each the four other conditions, Ref+3HP, evo1, evo2, and evo3, and the significance of differential expression for each gene was assessed by the *t*-test, as implemented in the genefilter package, followed by Benjamini & Hochberg *P*-value correction. Furthermore mean log 2 fold changes between the gene expression intensities for the four conditions (Ref+3HP, evo1, evo2, and evo3), and the gene intensities for the Ref were calculated for each gene. Additionally a consensus gene list was compiled based on the *P*-values for the three independent evolutions. Here the Fisher *P*-value combination method was used to determine a consensus *P*-value, and a consensus log fold change value was calculated as the mean of the log fold changes for the three independent evolutions. For each four conditions (Ref+3HP, evo1, evo2, and evo3), as well as for the consensus list, a set of top genes was defined as the top significant genes with a *P*-value less than 0.01 and absolute log fold change above 1.

The R gene set analysis package *piano* (version 1.2.10) (Väremo et al., 2013) was used to calculate the enrichment of GO-slim terms (*Saccharomyces* Genome Database, December 11, 2013) to be either distinctively up or down regulated in Ref+3HP, evo1, evo2, and evo3. The consensus *P*-values were used as gene-level statistics and log 2 fold changes were used as gene-level statistics and directions, respectively. The median (of the *P*-value gene-level statistics) was chosen as a gene-set statistic. Other suitable gene-set statics yielded qualitatively similar results. The significance of enrichment was determined via gene randomization and *P*-values were adjusted for multiple testing using the false discovery rate ('fdr' option).

2.6. Plasmids and strains construction

The plasmids and primers used in this study are listed in Tables S2 and S3, respectively. Manipulation of plasmid DNA and transformation of plasmids into *E. coli* were carried out according to standard procedures. Transformation of yeast cells was carried out according to Gietz and Woods, 2002 (Gietz and Woods, 2002).

The *sfa1*Δ and *ach1*Δ strains were constructed by replacing the target gene in the CEN.PK113-32D strain with the *KanMX* cassette. The gene fragments carrying the *KanMX* cassette and correct overhangs for *SFA1* and *ACH1* replacement were generated by PCR amplification using primers and templates as indicated in Table S3. The knock-out fragment was transformed into *S. cerevisiae* and transformants were selected on YPD+200 μg ml^{-1} G418 and confirmed by PCR.

The *SFA1*-alleles and *YJL068C* were amplified from genomic DNA of *S. cerevisiae* using primers and templates as described in Table S3. The amplified products were cloned together with promoter into pESC-LEU-USER plasmid by USER cloning (Jensen et al., 2014). The clones with correct inserts were confirmed by sequencing. The final plasmids were then transformed into different yeast strain backgrounds (Ref, *ach1*Δ, and *sfa1*Δ) and selected on synthetic complete medium without leucine (SC-Leu). The resulting strains are listed in Table S2.

The strain with *SFA1* allele replacement was constructed by replacing the *KanMX* cassette in the *sfa1*Δ strain with the corresponding upstream and downstream using the gene targeting strategy (Reid et al., 2002). The upstream fragment including the *SFA1* allele for each *SFA1* mutations, the downstream fragment of *SFA1* gene, the two fragments containing the 2/3 N-terminal and the C-terminal 2/3 part of a *Kluyveromyces lactis LEU2* (*KlLEU2*) marker were amplified using primers described in Table S3. To generate a complete gene targeting substrate, the upstream fragment including the *SFA1* allele for each *SFA1* mutations was fused to the 2/3 C-terminal of *KlLEU2* using primers described in Table S3. Similarly, the downstream fragment was fused to the 2/3 N-terminal of *KlLEU2*. The two fusion PCR fragments were co-transformed into the *sfa1*Δ strain and selected SC-Leu medium. The correct transformants were confirmed by PCR and the mutation in the *SFA1* gene was verified by sequencing. For the control strain, the *SFA1*^{wt} allele was introduced back to the *sfa1*Δ strain in an analogous way as other *SFA1* alleles.

The PCR site-directed mutagenesis was performed to replace the Cys276 residue with Gly, Ala, Val or Thr, and to replace the Met283 residue with Val or Ala using primers and templates listed in Table S3. The amplified products were treated with DpnI, gel-purified and subsequently transformed into *E. coli*. The correct mutations in the *SFA1* gene in the resulting plasmids were confirmed by sequencing.

The *SFA1* alleles were introduced back into the *sfa1*Δ strain as previously described with a slightly modification. Specifically, the upstream part of gene targeting substrate was generated by fusion

PCR using the *SFA1* upstream, the *SFA1*-allele and the 2/3 C-terminal of *KlLEU2* fragments as templates.

2.7. Modeling of Sfa1p

We built a homology model of Sfa1p using the HHpred server (http://toolkit.lmb.uni-muenchen.de/hhpred; PMID 15980461). The model was based on the experimental structure of *Arabidopsis thaliana* S-nitrosoglutatione reductase (3UKO), which exhibits 61% sequence identity to Sfa1p and covers residue 4-384 (of 386 residues; 98.4%). Following homology modeling, two zinc ions and a NAD(P)+ moiety were manually added from the template structure. The covalently linked substrate intermediate (S-(3-hydroxypropanoyl)-glutathione) was built by extending the corresponding substrate (S-hydroxymethl-glutathione) taken from the structure of human glutathione-dependent formaldehyde dehydrogenase (1MC5, PMID 12484756). The substrate intermediate was manually docked into the model (in a conformation similar to that found in 1MC5) and the entire complex was energy-minimized using the SYBYL software package. Finally, the monomer Sfa1p model was duplicated and arranged as a dimer by alignment to the template structure.

2.8. Growth test in 96-well microtiter plates

Pre-cultures were prepared by inoculating a single colony in 0.5 ml defined mineral medium (pH 3.5) containing 10 g l^{-1} 3HP in 96-deep well plate (Enzyscreen). The plate was incubated at 30 °C with 250 rpm agitation at 5 cm orbit cast overnight. 5 μl of the overnight cultures were inoculated into 100 μl of the same medium with or without 50 g l^{-1} 3HP in a 96-well flat bottom plate (Greiner). The plate was sealed with Breathe-Easy® sealing membrane (Sigma-Aldrich) and incubated at 30 °C with shaking in the Synergy™ MX microplate reader (BioTek) and the absorbance was measured at 600 nm wavelength every 15 min for 42 h. Experiments were done in triplicates, and the specific growth rate (h^{-1}) was calculated.

The effect of different pH values (pH 3.0–6.0) on the robustness of the 3HP-tolerant strains was performed by determining the maximal specific growth rate of the strains on defined mineral medium buffered with citrate–phosphate buffer. Experiments were set up as described above and were done in triplicates. To test whether mutation in the *SFA1* could confer tolerance to other compounds, the strains with or without overexpression of *SFA1* alleles were grown in defined mineral medium containing acetic acid (0–0.8%), lactic acid (0–4%), furfural (0–20 mM), methanol (0–30%), 1-propanol (0–15%), and 1-butanol (0–4%). For media containing acetic acid and lactic acid, the pH was adjusted to 3.5 instead of pH 6.0. The effect of GSH addition on 3HP tolerance in *S. cerevisiae* was performed by determining the growth of the strains on defined mineral medium (pH 3.5) with addition of 50 g l^{-1} 3HP and various concentrations of GSH (0–20 mM). The effect of GSH addition (5 mM) on the growth of other yeast strains in the presence of 50 g l^{-1} 3HP was performed as previously described except that defined mineral medium (pH 6.0) was used and the experiment was done at 25 °C. The effect of GSH addition on the growth of five *E. coli* strains in the presence of 20 g l^{-1} 3HP was investigated as following: a single colony from each strain was inoculated into 3 ml M9 medium and incubated at 250 rpm, 37 °C. 2 μl of the overnight cultures were used to inoculate 150 μl of M9, M9+20 g l^{-1} 3HP, and M9+20 g l^{-1} 3HP and 5 mM GSH in 96-well flat bottom plate. The pH of tested media was adjusted to pH 7.0. The 96-well plate was incubated with shaking in the ELx808™ Absorbance microplate reader (BioTek) at 37 °C and the absorbance was measured at 630 nm wavelength every 5 min for 22 h. Experiments were done in triplicates.

2.9. LC-MS analysis

Intracellular metabolites were extracted from cells by adding 1 ml of 0.1% (v/v) formic acid in water directly to the cells and the mixture was sonicated for 15 min. The cell mixture was pelleted and the supernatant was filtered through 0.2 μm syringe filter into a HPLC vial for further analysis. LC-MS data was collected on Orbitrap Fusion equipped with a Dionex brand Ultimate 3000 UHPLC pumping system (ThermoFisher Scientific, Waltham Ma). Samples were held in the autosampler at a temperature of 10 °C during the analysis. 25 μl injections of the sample were made onto a Discovery HS F5-5 HPLC column, with a 5 μm particle size, 4.6 mm i.d. and 150 mm long. The column was held at a temperature of 30.0 °C. The solvent system used was Solvent A "Water with 0.1% formic acid" and Solvent B "Acetonitrile with 0.1% formic". The Flow Rate was 0.6 ml/min with an Initial Solvent composition of %A=95, %B=5 held until 2.0 min, the solvent composition was then changed following a Linear Gradient until it reached %A=0.0 and %B=95 at 12 min. This was held until 14 min when the solvent was returned to the initial conditions and the column was re-equilibrated until 20 min. The column eluent flowed directly into the Heated ESI probe of the MS which was held at 325 °C and a voltage of 3500 V. Profile Data was collected in positive ion mode with Resolution setting of 30 K and Scan Range (m/z)=50–600. The other MS settings were as follows, Sheath Gas Flow Rate of 60 units, Aux Gas Flow Rate of 20 units, Sweep Gas Flow Rate of 5 units, Ion Transfer Tube Temp was 380 °C, Maximum Injection Time of 100 ms, S-Lens RF Level=60 V, using 1 Microscans and AGC Target=200,000 counts. The data was analyzed in a non-targeted manner using deconvolution software (AnalyzerPro, SpectralWorks Ltd, UK).

3. Results

3.1. Adaptive laboratory evolution of S. cerevisiae on 3HP and the resulting physiological and transcriptional changes

The growth of *S. cerevisiae* strain CEN.PK 113-7D is halved in the presence of 25 g l^{-1} 3HP and abolished when more than 40 g l^{-1} 3HP is added (Fig. S1). Using serial shake flask transfers for 48 days (≈200 generations) we obtained three parallel evolved cell lines capable of growing in defined mineral medium at pH 3.5 and a 3HP concentration of 50 g l^{-1} (Fig. 1A and B). Individual clones were isolated from the end-point cultures of the three independent evolution lines and designated as evo1, evo2 and evo3. The maximum specific growth rate μ_{max} at pH 3.5 and at 3HP concentration of 50 g l^{-1} was 0.18 h^{-1} for evo1 and evo2 and 0.20 h^{-1} for evo3 (Fig. S2), while in the absence of 3HP the μ_{max} was 0.33 h^{-1}, which is comparable to the μ_{max} of the reference strain. Two of the evolved strains, evo1 and evo3, could not metabolize ethanol and acetate after the exhaustion of glucose. In the presence of 3HP, acetate production was significantly increased in all three evolved strains compared to the reference. By HPLC measurement it was confirmed that the yeast strains were not capable of metabolizing 3HP, as concentrations of 3HP remained unchanged during the cultivation. Furthermore, the reference or evolved strains were unable to grow on 3HP as the sole carbon source (data not shown).

Genome-wide transcription analysis was performed on the three evolved strains and the Piano package for R (Väremo et al., 2013) was used to assess the enrichment of GO-slim terms in transcriptional changes. The evolved strains exposed to 50 g l^{-1} of 3HP showed a clear separation from the reference strain exposed to 3HP (10 g l^{-1}) in their transcriptional profiles (Fig. 1D). Interestingly a handful of genes involved in response to oxidative stress (e.g. *AHP1*, *YPR1*, *GLR1*, *GSH1*, *GRE3* etc.) were only differentially expressed in the evolved strains, indicating that these genes might

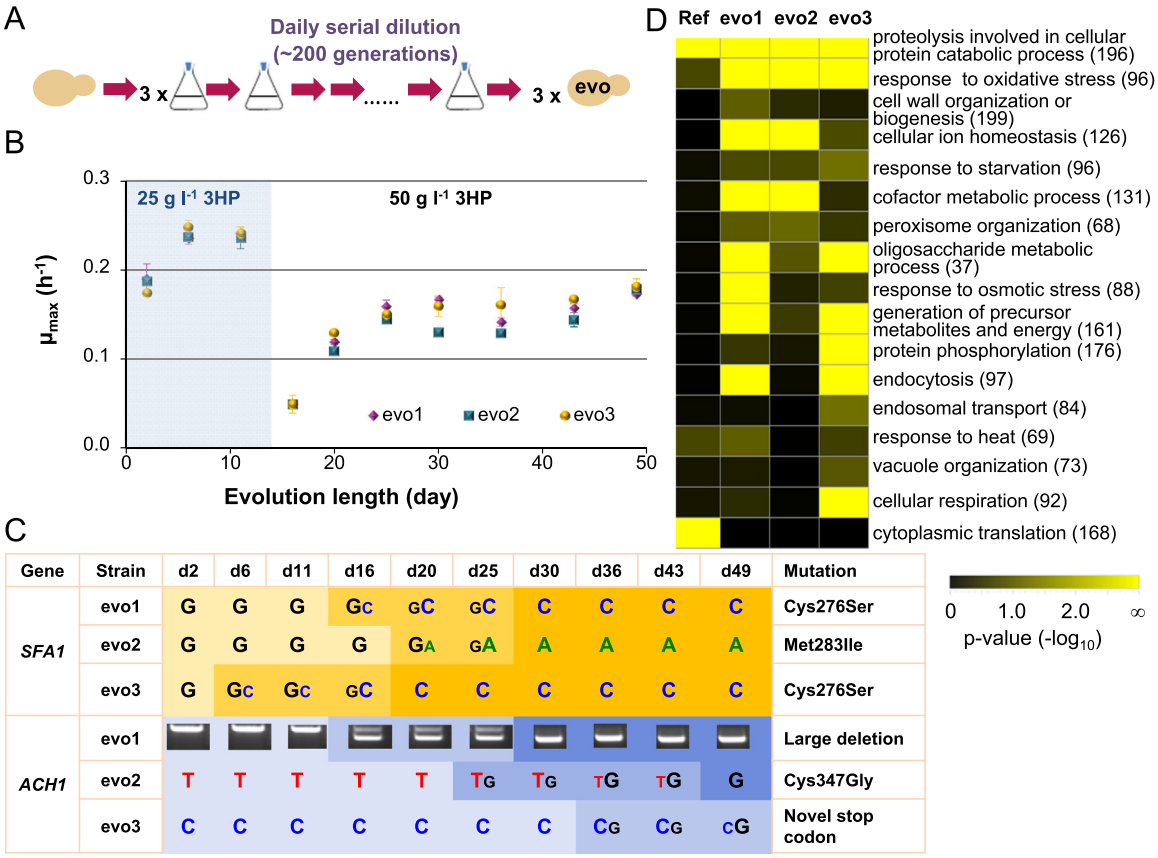

Gene	Strain	d2	d6	d11	d16	d20	d25	d30	d36	d43	d49	Mutation
SFA1	evo1	G	G	G	GC	GC	GC	C	C	C	C	Cys276Ser
	evo2	G	G	G	G	GA	GA	A	A	A	A	Met283Ile
	evo3	G	GC	GC	GC	C	C	C	C	C	C	Cys276Ser
ACH1	evo1											Large deletion
	evo2	T	T	T	T	T	TG	TG	TG	TG	G	Cys347Gly
	evo3	C	C	C	C	C	C	C	CG	CG	CG	Novel stop codon

Fig. 1. Evolutionary profile and changes in the phenotype, genotype and transcriptional profile of the evolved strains (evo1, evo2, and evo3). (A) Overview of the adaptive laboratory evolution procedure. (B) Phenotypic changes in the evolved strains: increased tolerance towards 3HP. Growth of cells sampled throughout evolution was tested in triplicates and standard deviations (SD) are shown by error bars. (C) Genotypic changes in the evolved strains. (D) Gene set enrichment analysis of evolved strains exposed to 50 g l^{-1} 3HP compare with the reference strain (Ref) exposed to 10 g l^{-1} 3HP. The Piano package for R was used to assess the enrichment of GO-slim terms in transcriptional changes. The heat map shows the significance of enrichment of GO-slim terms (process category) to be distinctively up-regulated i.e., containing predominantly positive logarithmic fold changes. The matrix contains only terms with $P < 0.01$ for at least one of the 3HP-treated strains and numbers in parentheses indicate total number of genes in the set.

be directly involved in the 3HP tolerance mechanism acquired during the adaptive evolution.

3.2. *Mutations in S-(hydroxymethyl)glutathione dehydrogenase (SFA1) and CoA-transferase (ACH1) were found in the three evolved cell lines by genome Re-sequencing*

The genomes of the three evolved strains were sequenced and mapped against the genome of the parent strain CEN.PK113-7D. Remarkably, two genes (*SFA1* and *ACH1*) contained non-silent mutations in all three evolved strains. The strains evo1 and evo3 had the same single point mutation in *SFA1*, where nucleotide at position 827 was changed from G to C (leading to a change in amino acid sequence: Cys276Ser), whereas a different point mutation, G849A (Met283Ile at the amino acid level) was observed in evo2 (Fig. 1C). Mutations in *ACH1* were different in the three evolved strains: a large deletion in evo1, a point mutation Cys347Gly in evo2 and a novel stop codon at position 488 in evo3. The onset and propagation of the different mutations in *SFA1* and *ACH1* in the populations of strains were analyzed by Sanger sequencing of *SFA1* and *ACH1* genes amplified from the intermediate populations sampled throughout evolution (Fig. 1C). The mutation in *SFA1* occurred in evo3 earlier than in the other strains, namely after 5 days of evolution (≈ 49 generations), in a medium containing 25 g l^{-1} 3HP, whereas *SFA1* was first mutated in evo1 and evo2 after shift to higher 3HP concentration (50 g l^{-1}) which occurred after 70–80 generations, at day 16–20 of evolution. Unlike *SFA1*, all mutations in *ACH1* occurred after the 3HP concentration was increased. After the appearance of mutations, a mixed population was observed for 25–70 generations (6–18 days) until the cells harboring the mutations predominated.

Six additional genes were found to carry mutations in only one of the evolved cell lines (Table S1). No insertions, gene duplications or modifications in the non-translated regions of the genome were found.

3.3. *Functional analysis reveals that mutations in SFA1 are the main cause of 3HP tolerance*

The genes that were found to carry mutations in the evolved strains made the basis for reverse metabolic engineering to obtain a 3HP-tolerant strain. We individually overexpressed or deleted the eight candidate genes in the reference strain and tested the effect of the genetic change on 3HP tolerance. Overexpression was performed by introducing an additional copy of the gene of interest under the control of a strong constitutive promoter, i.e. *pTEF1*. In addition to the overexpression of the native *SFA1* gene, overexpression of the mutated alleles was tested as well in the reference, *sfa1*Δ and *ach1*Δ strains. Overexpression of any of the *SFA1* alleles enabled growth of the cells in the presence of 50 g l^{-1} 3HP (Fig. 2A) with μ_{max} similar to that of the evolved strains. On the other hand, neither overexpression of *ACH1* gene (native and mutant alleles), nor overexpression or deletion of the other gene candidates identified from re-sequencing (Table S1) supported growth in the presence of 50 g l^{-1} 3HP. Deletion of *ACH1* abolished growth on ethanol, explaining the phenotype of the evo1 and evo3

strains that carried a large deletion and a novel stop codon in *ACH1*, respectively. This is in agreement with the work previously reported by Fleck and Brock (2009).

To investigate whether any of the *SFA1* mutant alleles could confer 3HP tolerance when expressed from the native promoter rather than strong constitute promoter, the native *SFA1* gene was replaced by either $SFA1^{C276S}$ or $SFA1^{M283I}$. The resulting strains had shorter lag phase on 25 g l^{-1} 3HP than the strain with the $SFA1^{wt}$ allele and they could grow on medium containing 3HP at concentrations above 40 g l^{-1}, whereas no growth was observed in the strain carrying the native *SFA1* allele (Fig. 2B). The effect of different pH values on the robustness of 3HP-tolerant strains was investigated. At 3HP concentration of 25 g l^{-1}, no significant difference in the robustness of the tolerant strains was observed at pH values between 3.0 and 5.0 (Fig. S3A and 3B). However, in medium containing 50 g l^{-1} 3HP, the growth inhibition was more pronounced at pH 3.0 and pH 5.0 than at pH 3.5 and pH 4.0 (Fig. S3C). In addition, we also tested whether mutation in *SFA1* could confer tolerance to other inhibitors, namely acetic acid, lactic acid, furfural, methanol, 1-propanol, and 1-butanol. The *SFA1* mutant alleles did not result in increased tolerance to any of the tested compounds (data not shown).

3.4. 3D structure model of the Sfa1 protein

S-(hydroxymethyl)glutathione dehydrogenase encoded by *SFA1* is a member of the class III alcohol dehydrogenase subfamily (EC:1.1.1.284), which encompasses bi-functional enzymes containing both alcohol dehydrogenase and glutathione-dependent formaldehyde dehydrogenase activity. To investigate the structural context of the mutations in *SFA1* identified in the evolved strains, we built a 3D structure model of Sfa1p based on an experimental structure of *A. thaliana* S-nitrosoglutatione reductase, which is a homo-dimer (3UKO) (Crotty, 2009). The model included a $NADP^+$ cofactor and a S-(3-hydroxypropanoyl)-glutathione fitted in a conformation similar to the one observed for the substrate in human glutathione-dependent formaldehyde dehydrogenase (1MC5). Each subunit contains two zinc-binding sites, one structural and one central to the catalytic function of the enzyme. An overview of the model with the mutations discussed in this work is shown in Fig. 2C. From the 3D model of Sfa1p it is evident that of the two observed mutations one (Cys276Ser) is found in the substrate-binding pocket interacting with the $NADP^+$ cofactor on the opposite side of the groove from the catalytic zinc, while the other (Met283Ile) is centrally placed in the dimerization lobe of the structure (approximately residues 268–326) in close proximity of the binding groove. Given that these two mutations presumably increase the ability of Sfa1p to accommodate and process the more bulky 3HP, we hypothesized that substitutions, which expand the substrate pocket, also increase the activity of Sfa1p towards 3HP. Indeed, we found that replacement of Cys276 residue with other small amino acids such as Thr, Gly, Val, Ala as well as replacing Met283 with either Val or Ala also conferred the 3HP tolerance phenotype (Fig. 2D).

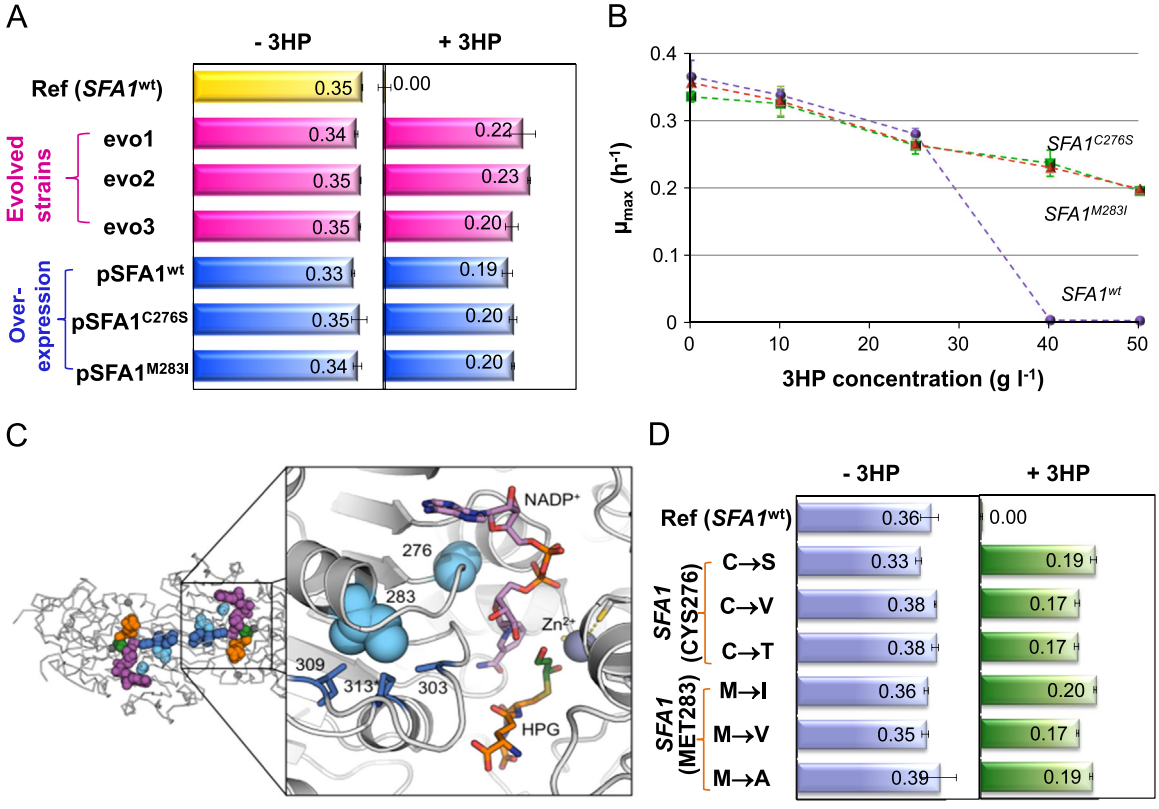

Fig. 2. The effect of *SFA1* on 3HP tolerance in yeast and characterization of Sfa1p. (A) 3HP tolerance in yeast conferred by overexpression of *SFA1* alleles, $pSFA1^{wt}$, $pSFA1^{C276S}$, and $pSFA1^{M283I}$, compared with the reference ($SFA1^{wt}$) and evolved strains (evo1, evo2, evo3) grown on defined mineral medium (pH 3.5) with or without 50 g l^{-1} of 3HP. (B) Growth of strains carrying mutated $SFA1^{C276S}$ and $SFA1^{M283I}$ alleles, respectively, compared with the strain carrying the $SFA1^{wt}$ (analogous to WT) grown on medium containing 3HP concentrations ranging from 0 to 50 g l^{-1}. Error bars represent the standard deviation (SD) in biological triplicates. (C) A 3D structure model of the Sfa1p from *S. cerevisiae*. The residues in the two positions found to be mutated in the evolved strains are shown in light blue (positions 276 and 283). Residues in three adjacent positions are shown in darker blue. The residue in position 313 reaches over (symmetrically) from the other subunit of the dimer (marked with an asterisk). The model also contains the $NAD(P)^+$ cofactor (purple) along with the putative, covalently linked substrate S-(3-hydroxypropanoyl)glutathione (HPG), consisting of a glutathione moiety (orange) and a 3-hydroxypropanoyl moiety (green). (D) The effect of mutations in Cys276 and Met283 residues on 3HP tolerance. Growth characterization of each strain was performed in triplicates and SD is given by error bars.

3.5. Proposed glutathione-dependent 3-hydroxypropionic aldehyde detoxification mechanism

The function of Sfa1p in formaldehyde detoxification has been proposed previously (Wehner et al., 1993). Formaldehyde spontaneously reacts with intracellular glutathione (GSH) to form S-hydroxymethylglutathione, which is then converted into S-formylglutathione by Sfa1p using $NAD(P)^+$ as cofactor. We hypothesized that in the yeast cells 3HP is converted into 3-hydroxypropionic aldehyde (3HPA) by aldehyde dehydrogenases, and that it is 3HPA that causes cellular toxicity and therefore has to be detoxified by a mechanism analogous to that of formaldehyde detoxification (Fig. 3).

In yeast the aldehyde dehydrogenases (Aldp) catalyze an important reaction of converting acetaldehyde into acetate, which is essential for generation of acetyl-CoA during growth on non-fermentable carbon source (e.g. ethanol). These enzymes also take care of oxidizing other harmful aldehydes (Yasokawa et al., 2010). We proposed that the enzyme does also catalyze the reverse reaction converting 3HP into 3HPA, which is supposedly highly toxic to yeast. In aqueous solutions 3HPA is present as a mixture of 3HPA, HPA-hydrate and HPA-dimer in a dynamic equilibrium. This mixture is generally referred to as reuterin, which is a wide-spectrum antimicrobial compound, active against Gram positive and Gram negative bacteria, fungi and protozoa (Axelsson et al., 2009). It can therefore be an advantage for yeast cells to convert reuterin into other less toxic compounds, and we here suggest that this detoxification involves spontaneous binding of 3HPA to GSH to form S-(3-hydroxypropanoyl)glutathione, which is then oxidized into S-(3-ketopropanoyl)glutathione by Sfa1p using $NAD(P)^+$ as a cofactor. Finally, the intermediate compound is hydrolyzed to 3HP with release of GSH by the S-formylglutathione hydrolase (encoded by *YJL068C*).

3.6. Deletion of ALD6 reduced susceptibility of yeast to 3HP

To investigate whether *ALDs* genes and their gene products are involved in 3HP detoxification mechanism, we tested the survival of *ALD* single deletion strains on high concentrations of 3HP. The *ald* deletion strains (*ald2*Δ, *ald3*Δ, *ald4*Δ, *ald5*Δ or *ald6*Δ) together with their parental strain BY4741 were grown in a medium containing either 25 or 50 g l^{-1} 3HP. No growth was observed for any of the strains grown on 50 g l^{-1} 3HP. Growth of the *ald6*Δ strain on 25 g l^{-1} 3HP was less inhibited by 3HP than the growth of the reference strain (4% inhibition instead of 31%) (Fig. 4A). These observations indicated a potential involvement of *ALDs* genes in 3HP detoxification and supported the proposed detoxification mechanism.

3.7. LC-MS analysis revealed that GSH involved in 3HP detoxification

To further evaluate if GSH is involved in the 3HP detoxification mechanism we measured the intracellular GSH level in the cells grown in a medium with or without 3HP by LC-MS analysis. The intracellular GSH level was similar in all strains, when quantified against the mass and retention time from an authentic glutathione standard (Fig. S4). However, upon examination of the mass spectral data files, we found groups of fragment ions that had masses within 10 ppm, indicative of the presence of GSH adducts. The identity of the GSH adducts could not be confirmed because of the lack of the standard. When relative quantitation (using the peaks with *m/z* of 306) was carried out on these samples, we observed a significant increase ($\approx$250 fold) in the GSH adduct concentration in the $SFA1^{C276S}$-allele exposed to 50 g l^{-1} 3HP compared to the reference strain (Fig. 4B). These results provide strong evidence that GSH play an important role in 3HP detoxification by binding to 3HPA.

3.8. Glutathione supplementation improved 3HP tolerance in several yeast species and in E. coli

Based on the proposed 3HP detoxification mechanism, we suggested that 3HP tolerance in *S. cerevisiae* might be improved by increasing the availability of GSH either by external addition or by improving its intracellular production. We therefore tested the effect of addition of external GSH for improving 3HP tolerance by *S. cerevisiae*. The strains with native or mutated *SFA1* alleles or with *sfa1* deletion were grown with or without 50 g l^{-1} 3HP and supplemented with varying concentrations of GSH (0–20 mM). The

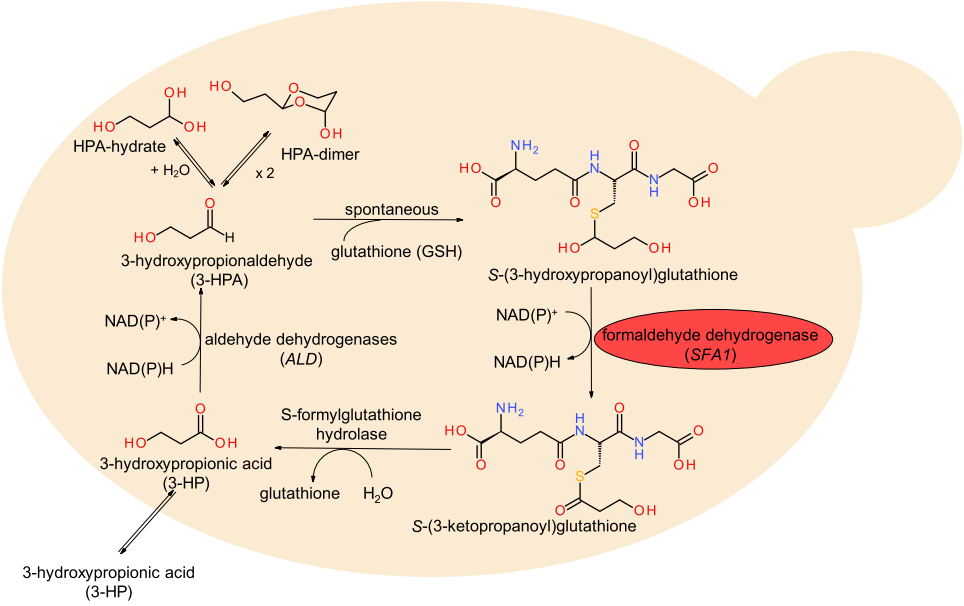

Fig. 3. The proposed glutathione-dependent mechanism of 3HP detoxification. Red circle indicates the reaction catalyzed by Sfa1p, an enzyme that carries mutations in the evolved 3HP-tolerant strains.

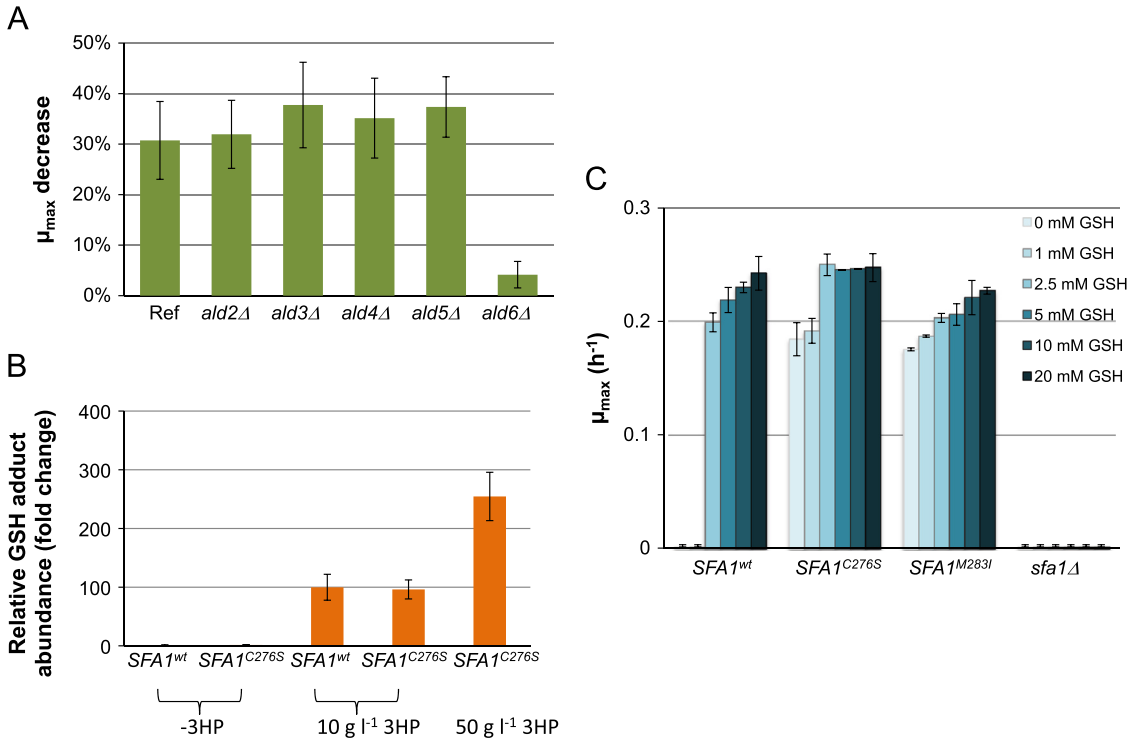

Fig. 4. Influence of aldehyde dehydrogenase and glutathione on 3HP tolerance in *S. cerevisiae*. (A) Growth characteristics of *ALD* deletion strains grown on SC medium with or without 25 g l^{-1} 3HP. (B) LC-MS analysis of intracellular GSH adduct level from *S. cerevisiae* carrying the native (*SFA1*^{wt}) or mutated *SFA1* gene (*SFA1*^{C276S}) grown on defined mineral medium (pH 3.5) with or without 3HP. Data represented as a fold change of GSH abundance relative to the *SFA1*^{wt} strain (no 3HP). (C) The effect of GSH addition on 3HP tolerance in *S. cerevisiae* carrying the *SFA1*-alleles and the *sfa1*Δ strain grown on medium containing 50 g l^{-1} 3HP. Error bars represent SD of biological triplicates.

concentrations of GSH above 2.5 mM restored the growth of the *S. cerevisiae* in the presence of 50 g l^{-1} 3HP so the μ_{max} was slightly higher than that of the *SFA1*-mutated strains grown without GSH supplement (Fig. 4C). Furthermore, GSH addition also further improved the growth rate of the strain carrying the *SFA1*^{C276S} or *SFA1*^{M283I} alleles. The growth of the *sfa1*Δ strain could not be restored by addition of GSH. In addition, GSH had no significant effect on the growth of the strains in the absence of 3HP. These findings further confirm the connection between tolerance to 3HP, GSH and Sfa1p.

In addition to *S. cerevisiae*, we demonstrated that addition of GSH also improves the tolerance of several other yeast species to 3HP. Addition of 5 mM GSH enabled growth of 3HP-sensitive strains (*S. cerevisiae*, *Saccharomyces kluyveri* and *K. lactis*) in the presence of 50 g l^{-1} 3HP and improved the μ_{max} of the strains that were naturally tolerant to 3HP (*Kluyveromyces marxianus*, *Yarrowia lipolytica*, *Cyberlindnera jadinii, Schizosaccharomyces pombe*, *Torulaspora delbrueckii* and *Rhodotorula minuta*) (Fig. S5A). Similarly supplementation of 5 mM GSH restored the growth of five *E. coli* strains, i.e. W3110, CROOKS, W, DH5α and BL21, in M9 medium supplemented with 20 g l^{-1} 3HP and improved the growth of MG1655 strain (Fig. S5B). These results suggest that our identified mechanism for improving tolerance to 3HP may be similar in different microorganisms.

3.9. S-formylglutathione hydrolase is involved in 3HP detoxification

In the proposed 3HP detoxification pathway, we suggest that the intermediate S-(3-ketopropanoyl)glutathione derived from Sfa1p activity is further converted into 3HP by the S-formylglutathione hydrolase encoded by *YJL068C*. Therefore, the role of S-formylglutathione hydrolase in 3HP detoxification was investigated. The *YJL068C* gene was either deleted or overexpressed in strains expressing either native or *SFA1* alleles and tested for 3HP tolerance on medium containing 25 g l^{-1} 3HP. The concentration of 25 g l^{-1} 3HP was used because the *SFA1*^{wt} background strain could not tolerate 50 g l^{-1} 3HP. Deletion of *YJL068C* gene decreased μ_{max} on 3HP by 55% in the strain with *SFA1*^{wt} background and by 10–20% in the strains with *SFA1*^{C276S} or *SFA1*^{M283I} (Fig. S6A). Overexpression of *YJL068C* also had a negative effect on 3HP tolerance, with 30% and 10% decrease in μ_{max} in *SFA1*^{wt} and *SFA1*^{C276S} backgrounds correspondingly (Fig. S6B). Deletion or overexpression of *YJL068C* might affect the turnover rate of GSH recycling and the overall detoxification mechanism.

4. Discussion

In this study, we demonstrated that adaptive laboratory evolution is a powerful method to generate *S. cerevisiae* strains tolerant to a heterologous product (3HP) and also to provide insights about possible mechanism for product toxicity and detoxification. By re-sequencing the genomes of the evolved 3HP-tolerant strains we found mutations in a total of 8 genes, of which *SFA1* and *ACH1* were mutated in all three evolved strain lines. By inverse metabolic engineering we could reconstitute the 3HP-tolerant phenotype to the level of that of the evolved strains by overexpressing *SFA1* or by point-mutating *SFA1* to substitute amino acids in positions Cys276 or Met283 to smaller ones such as Gly, Ala or Ile. It appeared that the expression level of the native *SFA1* was insufficient to confer tolerance to 3HP. However the mutations likely increased the activity of the enzyme towards the 3HP-derived compound and hence even the native levels of the gene expression were sufficient for tolerance.

We hypothesized that 3HP can be converted in the yeast cells into 3HPA by aldehyde dehydrogenases. Several hypotheses for

toxicity of 3HPA have been proposed. The ability of the dimeric form of 3HPA to act as competitive inhibitor of ribonucleotides makes it an inhibitor of DNA synthesis that can lead to cell death. Alternatively, 3HPA is highly reactive and can inhibit the activity of thioredoxin, a protein participating in cellular redox regulation (Barbirato et al., 1996; Rasch, 2002). Furthermore, 3HPA might interact with thiol groups and primary amines and therefore could inactivate proteins and small molecules containing these thiol groups (Vollenweider and Lacroix, 2004). Recently, Schaefer et al. (2010) provided the evidence that reuterin induces oxidative stress in *E. coli* cells by modifying thiol groups of proteins and small molecules. Gene expression analysis of *E. coli* in response to exposure to reutein revealed an increased expression of genes that encode proteins containing thiol groups and genes involved in the oxidative stress response. In our case, gene expression analysis of the evolved strains exposed to 3HP also revealed significant changes in genes involved in oxidative stress and redox balance, which strongly indicated that the cells were undergoing oxidative stress mediated by interaction of the aldehyde form of reuterin and thiol groups of small molecules and proteins.

It has been reported that certain mutations in *SFA1* or *SFA1* deletion can decrease resistance to formaldehyde, S-nitrosoglutathione, and peroxynitrite (Fernández et al., 2003). Other recently reported mutations in the *SFA1* gene (Val208Ile, Ala303Thr, Met283Ile, Ile309Met, and Pro313Ala) have been shown to improve formaldehyde tolerance (Zhang et al., 2013). Two of these mutations (Val208Ile and Ala303Thr) are located in the active site of Sfa1p. Interestingly, mutations Ala303Thr, Ile309Met, and Pro313Ala (reaching over from the other monomer, Fig. 2C) form a tight cluster around Met283 and thus seem to identify a mutational hotspot with the ability to modulate the function of Sfa1p.

In our 3D model, both Cys276 and Met283 are located in the vicinity of the substrate-binding pocket. By replacing these amino acid residues with other smaller amino acids, Sfa1p apparently becomes more efficient at processing 3HPA. This suggests a widening of the substrate-binding pocket, since 3HPA is significantly larger than formaldehyde. Other possibilities, which cannot be ruled out based on our data include changes in enzyme dynamics and thus active site accessibility or an increased rate of release of the product (or cofactor) from the binding site due to mild destabilization of the complex.

We were wondering whether some specific mutations in *SFA1* gene are conserved among distantly related organisms. We therefore aligned Sfa1p orthologs from several yeast species, *A. thaliana*, *E. coli* and *Lactobacilli* species, which naturally possess high tolerance to reuterin (Fig. S7). Surprisingly, the position corresponding to Sfa1p residue 276, was conserved across all the analyzed *Lactobacilli* and contained Thr instead of Cys. Another position, 283 was also conserved in *Lactobacilli* with Ile or Val. Both *E. coli* and yeast had Met in position 283. These findings may point towards the similarity for the mechanism of 3HPA tolerance across different species. However, some yeast strains (i.e. *C. jadinii*, *S. pombe*, *T. delbrueckii*, *K. marxianus, Y. lipolytica and R. minuta)* are naturally tolerant to 3HP while they do not contain mutation in the SFA1p. The robustness of these strains to high 3HP concentration might occur by other mechanism, where higher expression level of the *SFA1* gene or higher glutathione regeneration could be some of the possibilities.

We observed that GSH could rescue or improve the growth of several yeast species and of *E. coli* in the presence of 3HP. GSH plays an important role in several stress response mechanisms such as protection against oxidative stress, xenobiotics, and heavy metal stress, and maintaining the cellular redox homeostasis (Carmel-Harel and Storz, 2000; Meister and Anderson, 1983; Penninckx, 2002). We proposed that GSH is involved in 3HPA detoxification by trapping the toxic 3HPA into S-(3-hydroxypropanoyl)glutathione, which can then become the substrate for Sfa1p. It was previously reported that several facultative anaerobic Gram positive bacteria (e.g. *Lactococcus lactis* subsp. *lactis, Streptococcus agalactiae* ATCC 12927) and the native reuterin producers such as *L. reuteri* can synthesize significant amount of GSH (Cleusix et al., 2007; Vollenweider et al., 2010).

The proposed 3HP tolerance mechanism was quite different from the common tolerance mechanism to weak organic acids. In general, the toxicity of organic acids depends on their hydrophobicity and p*K*a. At external pH below p*K*a, the equilibrium will move toward the undissociated form (RCOOH), which can cross the cell membrane by simple diffusion. Once inside the higher pH environment of the cytosol, the acid will dissociate and generate protons and the acid anion ($RCOO^-$). The acid anion cannot readily permeate across the plasma membrane and will accumulate inside the cell, which can interfere with several metabolic pathways and cause severe oxidative stress (Casal et al., 2008). To overcome toxicity generated by carboxylic acids, one could improve the secretion of carboxylic acid to reduce anion accumulation. For example, enhancement of acetic acid tolerance could be obtained by overexpressing *HAA1* gene, a transcriptional activator of multiple membrane transporters (Tanaka et al., 2012).

The effect of engineering 3HP tolerance into 3HP-producing yeast strains is currently under investigation. We observed no negative effect of overexpressing mutated alleles of *SFA1* on 3HP production (our unpublished results); however positive effects will likely first be seen at higher 3HP titers, preferably above 50 g l^{-1}.

5. Conclusion

This study shows how laboratory evolution, followed by functional and systems-level analysis, enabled uncovering glutathione-dependent mechanism behind 3HP detoxification. Glutathione-dependent detoxification of 3HP was not limited to the studied organism (*S. cerevisiae*), but was conserved across several yeast spp. and *E. coli*. The tolerance to 3HP could be reverse engineered into *S. cerevisiae* host, which is valuable for biological production of 3HP, one of the most interesting building block chemicals for sustainable polymer production. Finally our results suggest that 3HP toxicity may be mediated by 3HPA (reuterin), an antimicrobial compound important for maintaining healthy gut flora in humans and animals.

Acknowledgments

The research was founded by grant from The Novo Nordisk Foundation.

Appendix A. Supporting information

Supplementary data associated with this article can be found in the online version at http://dx.doi.org/10.1016/j.ymben.2014.09.004.

References

Abyzov, A., Urban, A.E., Snyder, M., Gerstein, M., 2011. CNVnator: an approach to discover, genotype, and characterize typical and atypical CNVs from family and population genome sequencing. Genome Res. 21, 974–984.

Axelsson, L.T., Chung, T.C., Dobrogosz, W.J., Lindgren, S.E., 2009. Production of a broad spectrum antimicrobial substance by *Lactobacillus reuteri*. Microb. Ecol. Health Dis. 2, 131–136.

Barbirato, F., Grivet, J.P., Soucaille, P., Bories, A., 1996. 3-Hydroxypropionaldehyde, an inhibitory metabolite of glycerol fermentation to 1,3-propanediol by enterobacterial species. Appl. Environ. Microbiol. 62, 1448–1451.

Carmel-Harel, O., Storz, G., 2000. Roles of the glutathione- and thioredoxin-dependent reduction systems in the *Escherichia coli* and *Saccharomyces cerevisiae* responses to oxidative stress. Annu. Rev. Microbiol. 54, 439–461.

Casal, M., Paiva, S., Queirós, O., Soares-Silva, I., 2008. Transport of carboxylic acids in yeasts. FEMS Microbiol. Rev. 32, 974–994.
Chen, Y., Bao, J., Kim, I.K., Siewers, V., Nielsen, J., 2014. Coupled incremental precursor and co-factor supply improves 3-hydroxypropionic acid production in *Saccharomyces cerevisiae*. Metab. Eng. 22, 104–109.
Cleusix, V., Lacroix, C., Vollenweider, S., Duboux, M., Blay, G.L., 2007. Inhibitory activity spectrum of reuterin produced by *Lactobacillus reuteri* against intestinal bacteria. BMC Microbiol. 7, 101.
Crotty, J., 2009. Crystal structures and kinetics of S-nitrosoglutathione reductase from *Arabidopsis thaliana* and Human (Ph.D. dissertation). The University of Arizona, Tuscon, USA.
Danecek, P., Auton, A., Abecasis, G., Albers, C.A., Banks, E., DePristo, M.A., Handsaker, R.E., Lunter, G., Marth, G.T., Sherry, S.T., McVean, G., Durbin, R., 2011. The variant call format and VCFtools. Bioinformatics 27, 2156–2158.
Dhar, R., Sägesser, R., Weikert, C., Yuan, J., Wagner, A., 2011. Adaptation of *Saccharomyces cerevisiae* to saline stress through laboratory evolution. J. Evolut. Biol. 24, 1135–1153.
Dragosits, M., Mattanovich, D., 2013. Adaptive laboratory evolution - principles and applications for biotechnology. Microb. Cell Factories 12, 64.
Fernández, M.R., Biosca, J.A., Parés, X., 2003. S-nitrosoglutathione reductase activity of human and yeast glutathione-dependent formaldehyde dehydrogenase and its nuclear and cytoplasmic localisation. Cell. Mol. Life Sci. 60, 1013–1018.
Fiume, M., Smith, E.J.M., Brook, A., Strbenac, D., Turner, B., Mezlini, A.M., Robinson, M.D., Wodak, S.J., Brudno, M., 2012. Savant genome browser 2: visualization and analysis for population-scale genomics. Nucleic Acids Res. 40, W615–W621.
Fleck, C.B., Brock, M., 2009. Re-characterisation of *Saccharomyces cerevisiae* Ach1p: fungal CoA-transferases are involved in acetic acid detoxification. Fungal Genet. Biol. 46, 473–485.
Gietz, R.D., Woods, R.A., 2002. Transformation of yeast by lithium acetate/single-stranded carrier DNA/polyethylene glycol method. Methods Enzymol. 350, 87–96.
Gokarn, R.R., Selifonova, O.V., Jessen, H.J., Gort, S.J., Selmer, T., Buckel, W. 3-hydroxypropionic acid and other organic compounds. Patent US 7186541 B2; 2007.
Hong, K.K., Nielsen, J., 2012. Recovery of phenotypes obtained by adaptive evolution through inverse metabolic engineering. Appl. Environ. Microbiol. 78, 7579–7586.
Hong, K.-K., Vongsangnak, W., Vemuri, G.N., Nielsen, J., 2011. Unravelling evolutionary strategies of yeast for improving galactose utilization through integrated systems level analysis. Proc. Natl. Acad. Sci. USA 108, 12179–12184.
Jensen, N.B., Strucko, T., Kildegaard, K.R., David, F., Maury, J., Mortensen, U.H., Forster, J., Nielsen, J., Borodina, I., 2014. EasyClone: method for iterative chromosomal integration of multiple genes in *Saccharomyces cerevisiae*. FEMS Yeast Res. 14, 238–248.
Kumar, V., Ashok, S., Park, S., 2013. Recent advances in biological production of 3-hydroxypropionic acid. Biotechnol. Adv. 31, 945–961.
Li, H., Handsaker, B., Wysoker, A., Fennell, T., Ruan, J., Homer, N., Marth, G., Abecasis, G., Durbin, R., 2009. The sequence alignment/Map format and SAMtools. Bioinformatics 25, 2078–2079.
Li, Y., Zheng, H., Luo, R., Wu, H., Zhu, H., Li, R., Cao, H., Wu, B., Huang, S., Shao, H., Ma, H., Zhang, F., Feng, S., Zhang, W., Du, H., Tian, G., Li, J., Zhang, X., Li, S., Bolund, L., Kristiansen, K., de Smith, A.J., Blakemore, A.I.F., Coin, L.J.M., Yang, H., Wang, J., Wang, J., 2011. Structural variation in two human genomes mapped at single-nucleotide resolution by whole genome de novo assembly. Nat. Biotechnol. 29, 723–730.
Liao, H., Gokarn, R.R., Gort, S.J., Jessen, H.J., Selifonova, O.V. Production of 3-hydroxypropionic acid using beta-alanine/pyruvate aminotransferase. Patent Appl. US 2010/0267115 A1; 2010.
Lynch, M.D., Warnecke, T., Gill, R.T., 2007. SCALEs: multiscale analysis of library enrichment. Nat. Methods 4, 87–93.
McKenna, A., Hanna, M., Banks, E., Sivachenko, A., Cibulskis, K., Kernytsky, A., Garimella, K., Altshuler, D., Gabriel, S., Daly, M., DePristo, M.A., 2010. The genome analysis toolkit: a mapReduce framework for analyzing next-generation DNA sequencing data. Genome Res. 20, 1297–1303.
Meister, A., Anderson, M.E., 1983. Glutathione. Annu. Rev. Biochem. 52, 711–760.
Oud, B., Flores, C.L., Gancedo, C., Zhang, X., Trueheart, J., Daran, J.M., Pronk, J.T., van Maris, A.J., 2012. An internal deletion in *MTH1* enables growth on glucose of pyruvate-decarboxylase negative, non-fermentative *Saccharomyces cerevisiae*. Microb. Cell Factories 11, 131.
Penninckx, M.J., 2002. An overview on glutathione in *Saccharomyces* versus non-conventional yeasts. FEMS Yeast Res. 2, 295–305.
Rasch, M., 2002. The influence of temperature, salt and pH on the inhibitory effect of reuterin on *Escherichia coli*. Int. J. Food Microbiol. 72, 225–231.
Reid, R.J.D., Lisby, M., Rothstein, R., 2002. Cloning-free genome alterations in *Saccharomyces cerevisiae* using adaptamer-mediated PCR. Methods Enzymol. 350, 258–277.
Schaefer, L., Auchtung, T.A., Hermans, K.E., Whitehead, D., Borhan, B., Britton, R.A., 2010. The antimicrobial compound reuterin (3-hydroxypropionaldehyde) induces oxidative stress via interaction with thiol groups. Microbiology 156, 1589–1599.
Simpson, J.T., Wong, K., Jackman, S.D., Schein, J.E., Jones, S.J.M., Birol, I., 2009. ABySS: a parallel assembler for short read sequence data. Genome Res. 19, 1117–1123.
Suthers, P., Cameron, D. Production of 3-hydroxypropionic acid in recombinant organisms. Patent US 6852517 B1;2006.
Tanaka, K., Ishii, Y., Ogawa, J., Shima, J., 2012. Enhancement of acetic acid tolerance in *Saccharomyces cerevisiae* by overexpression of the *HAA1* gene, encoding a transcriptional activator. Appl. Environ. Microbiol. 78, 8161–8163.
Valdehuesa, K.N.G., Liu, H., Nisola, G.M., Chung, W.J., Lee, S.H., Park, S.J., 2013. Recent advances in the metabolic engineering of microorganisms for the production of 3-hydroxypropionic acid as C3 platform chemical. Appl. Microbiol. Biotechnol. 97, 3309–3321.
Väremo, L., Nielsen, J., Nookaew, I., 2013. Enriching the gene set analysis of genome-wide data by incorporating directionality of gene expression and combining statistical hypotheses and methods. Nucleic Acids Res. 41, 4378–4391.
Vollenweider, S., Evers, S., Zurbriggen, K., Lacroix, C., 2010. Unraveling the hydroxypropionaldehyde (HPA) system: an active antimicrobial agent against human pathogens. J. Agric. Food Chem. 58, 10315–10322.
Vollenweider, S., Lacroix, C., 2004. 3-hydroxypropionaldehyde: applications and perspectives of biotechnological production. Appl. Microbiol. Biotechnol. 64, 16–27.
Warnecke, T.E., Lynch, M.D., Karimpour-Fard, A., Lipscomb, M.L., Handke, P., Mills, T., Ramey, C.J., Hoang, T., Gill, R.T., 2010. Rapid dissection of a complex phenotype through genomic-scale mapping of fitness altering genes. Metab. Eng. 12, 241–250.
Warnecke, T.E., Lynch, M.D., Karimpour-Fard, A., Sandoval, N., Gill, R.T., 2008. A genomics approach to improve the analysis and design of strain selections. Metab. Eng. 10, 154–165.
Warnecke, T.E., Lynch, M.D., Lipscomb, M.L., Gill, R.T., 2012. Identification of a 21 amino acid peptide conferring 3-hydroxypropionic acid stress-tolerance to *Escherichia coli*. Biotechnol. Bioeng. 109, 1347–1352.
Wehner, E.P., Rao, E., Brendel, M., 1993. Molecular structure and genetic regulation of *SFA*, a gene responsible for resistance to formaldehyde in *Saccharomyces cerevisiae*, and characterization of its protein product. Mol. Gen. Genet. 237, 351–358.
Yasokawa, D., Murata, S., Iwahashi, Y., Kitagawa, E., Nakagawa, R., Hashido, T., Iwahashi, H., 2010. Toxicity of methanol and formaldehyde towards *Saccharomyces cerevisiae* as assessed by DNA microarray analysis. Appl. Biochem. Biotechnol. 160, 1685–1698.
Zhang, H., Zeidler, A.F.B., Song, W., Puccia, C.M., Malc, E., Greenwell, P.W., Mieczkowski, P.A., Petes, T.D., Argueso, J.L., 2013. Gene copy-number variation in haploid and diploid strains of the yeast *Saccharomyces cerevisiae*. Genetics 193, 785–801.
Zhang, J., Wang, J., Wu, Y., 2012. An improved approach for accurate and efficient calling of structural variations with low-coverage sequence data. BMC Bioinform. 13, 1–11.